CORE
Metadata, citation and similar papers at core.ac.uk
Provided by Repository@USM

ENHANCEMENT IN RESISTIVITY RESOLUTION BASED ON DATA AMALGAMATION TECHNIQUE

ANDY ANDERSON ANAK BERY

UNIVERSITI SAINS MALAYSIA

2015

ENHANCEMENT IN RESISTIVITY RESOLUTION BASED ON DATA AMALGAMATION TECHNIQUE

By

ANDY ANDERSON ANAK BERY

Thesis submitted in fulfilment of
the requirements for the degree of
Doctor of Philosophy

DECEMBER 2015

ACKNOWLEDGMENTS

First and foremost, praises and thanks to the Almighty God for showers of blessing throughout my PhD study to complete the research successfully.

I would like to express my deep sincere thanks and gratitude to my main supervisor, Associate Professor Dr. Rosli Saad, for his motivations, advices, and immense knowledge. His guidance and kindly supervision helped me in completing my PhD study. I also would like to express my sincere gratitude to my co-supervisor Dr. Nordiana Mohd Muztaza for her helps and suggestions. Special thanks to Professor Dato' Dr. Mohd Mokhtar Saidin, Director of Centre for Global Archaeological Research (CGAR) for permission conducting research allowing the use of data and borehole records.

Secondly, I would like to give my appreciation to all the laboratory assistants, Mr. Yaakub Othman, Mr. Shahil Ahmad Khosaini and Mr. Azmi Abdullah that helps and guided me throughout period of my PhD study.

I would like to thank and give my appreciation to colleagues Dr. Nur Azwin Ismail and Dr. Noer El Hidayah Ismail. Thanks also to postgraduates, Mr. Yakubu Mingyi Samuel, Mr. Kiu Yap Chong, Mr. Mark Jinmin, Mr. Ragu Ragava Rao Satinaranan and lastly Madam. Nur Aminuda Kamaruddin. I would like to send my deep sincere thanks to them all for helps and supports.

I also would like to thanks Kementerian Pelajaran Malaysia and Universiti Sains Malaysia for the Skim Latihan Akademik Bumiputera (SLAB) scholarship and financial support throughout period of my PhD study.

Last but not least, my sincere thanks and profound appreciation to my beloved parents Mr. Bery Sidos and Mdm. Pauline Pungga, my sister Eva Diana Bery and my brother Jeff Steven Bery who have provided me with their prayers, encouragements and supports throughout my PhD study.

TABLE OF CONTENTS

		Page
Acknowledgments		ii
Table of Contents		iii
List of Tables		vi
List of Figures		vii
List of Symbols		xi
List of Abbreviations		xii
Abstrak		xiii
Abstract		xv
CHAPTER 1: INTRODUCTION		**1**
1.0	Background	1
1.1	Problem statements	3
1.2	Research objectives	4
1.3	Motivation and research novelty	5
1.4	Layout of thesis	6
CHAPTER 2: LITERATURE REVIEW		**8**
2.0	Introduction	8
2.1	Electrical resistivity theory	9
2.2	Basic concept of 2-D resistivity imaging	11
2.3	The general four-electrode method	13
2.4	Selecting electrode array for 2-D resistivity survey	15
	2.4.1 D-D array	16
	2.4.2 P-D array	17
	2.4.3 W array	18

2.4.4 W-S array 19
2.5 Electrode arrays 20
2.6 Inversion of resistivity data 21
2.7 Previous studies 23
2.7.1 Critical comments on resistivity data processing technique 27
2.8 Chapter summary 32

CHAPTER 3: RESEARCH METHODOLOGY 33

3.0 Introduction 33
3.1 Research methodology flowcharts 34
3.2 Phase 1: 2-D computerized models and field model 37
3.2.1 Forward modelling 37
3.2.2 Geological models test 38
3.2.2.1 A block model 38
3.2.2.2 Two blocks model 39
3.2.2.3 Contact zone model 40
3.2.2.4 Vertical dyke model 40
3.2.2.5 Fault model 41
3.2.3 The DLA technique for two different arrays 42
3.2.4 Field model 42
3.2.5 The DLA technique for field model data 43
3.2.6 Inversion modelling 43
3.3 Phase 2: The numerical comparative assessment 44
3.4 Phase 3: Validation of the DLA technique 46
3.4.1 Minden, USM, Penang 47
3.4.2 Bukit Bunuh, Perak 48
3.5 Chapter summary 50

CHAPTER 4: RESULTS AND DISCUSSIONS **51**
4.0 Introduction 51
4.1 Results of 2-D computerized models 51
4.1.1 A block model 51
4.1.2 Two blocks model 61
4.1.3 Contact zone model 71
4.1.4 Vertical dyke model 81
4.1.5 Fault model 91
4.1.6 The numerical comparative assessment 101
4.1.7 Conclusion of 2-D computerized models 103
4.2 Field model study 109
4.2.1 The buried bunker, USM, Penang 109
4.2.2 The numerical comparative assessment 119
4.2.3 Conclusion of field model 121
4.3 Field studies 123
4.3.1 Minden, USM, Penang 123
4.3.2 Bukit Bunuh, Perak 124
4.4 Chapter summary 126

CHAPTER 5: CONCLUSION AND RECOMMENDATIONS **127**

5.0 Conclusion 127
5.1 Recommendations for future research 129

REFERENCES 130

LIST OF TABLES

Page

Table 3.1	Parameters of forward modelling for four different arrays used.	38
Table 4.1	The numerical comparative assessment for a block model.	104
Table 4.2	The numerical comparative assessment for two blocks model.	105
Table 4.3	The numerical comparative assessment for contact zone model.	106
Table 4.4	The numerical comparative assessment for vertical dyke model	107
Table 4.5	The numerical comparative assessment for fault model.	108
Table 4.6	The numerical comparative assessment for the buried bunker.	122

LIST OF FIGURES

		Page
Figure 2.1	Common electrodes array for resistivity measurement.	12
Figure 2.2	Arrangement of four-electrode in electrical resistivity method.	13
Figure 2.3	Electrode's arrangement for D-D array.	16
Figure 2.4	Electrode's arrangement for P-D array.	17
Figure 2.5	Electrode's arrangement for W array.	18
Figure 2.6	Electrode's arrangement for W-S array	19
Figure 2.7	Common arrays used in resistivity and their geometric factors.	21
Figure 3.1	Research methodology flowchart for the Phase 1.	35
Figure 3.2	Research methodology flowchart for the Phase 2.	36
Figure 3.3	The synthetic model showing a block embedded in homogenous medium.	39
Figure 3.4	The synthetic model showing two blocks embedded in homogenous medium.	39
Figure 3.5	The synthetic model showing contact zone attached with homogenous medium.	40
Figure 3.6	The synthetic model showing vertical dyke crossed with homogenous medium.	41
Figure 3.7	The synthetic model showing fault attached with homogenous medium.	41
Figure 3.8	Penang Island geological map.	48
Figure 3.9	Geological map of Bukit Bunuh study area with blue triangle.	49
Figure 4.1	The block model results given by D-D array.	52
Figure 4.2	The block model results given by P-D array.	53
Figure 4.3	The block model results given by W array.	54
Figure 4.4	The block model results given by W-S array.	55
Figure 4.5	The block model results given by the DLA technique of (D-D+P-D) arrays.	56
Figure 4.6	The block model results given by the DLA technique of (D-D+W) arrays.	57

Figure 4.7	The block model results given by the DLA technique of (D-D+W-S) arrays.	58
Figure 4.8	The block model results given by the DLA technique of (P-D+W) arrays.	59
Figure 4.9	The block model results given by the DLA technique of (P-D+W-S) arrays.	60
Figure 4.10	The block model results given by the DLA technique of (W+W-S) arrays.	61
Figure 4.11	The two blocks model results given by D-D array.	62
Figure 4.12	The two blocks model results given by P-D array.	63
Figure 4.13	The two blocks model results given by W array.	64
Figure 4.14	The two blocks model results given by W-S array.	65
Figure 4.15	The two blocks model results given by the DLA technique of (D-D+P-D) arrays.	66
Figure 4.16	The two blocks model results given by the DLA technique of (D-D+W) arrays.	67
Figure 4.17	The two blocks model results given by the DLA technique of (D-D+W-S) arrays.	68
Figure 4.18	The two blocks model results given by the DLA technique of (P-D+W) arrays.	69
Figure 4.19	The two blocks model results given by the DLA technique of (P-D+W-S) arrays.	70
Figure 4.20	The two blocks model results given by the DLA technique of (W+W-S) arrays.	71
Figure 4.21	The contact zone model results given by D-D array.	72
Figure 4.22	The contact zone model results given by P-D array.	73
Figure 4.23	The contact zone model results given by W array.	74
Figure 4.24	The contact zone model results given by W-S array.	75
Figure 4.25	The contact zone model results given by the DLA technique of (D-D+P-D) arrays.	76
Figure 4.26	The contact zone model results given by the DLA technique of (D-D+W) arrays.	77
Figure 4.27	The contact zone model results given by the DLA technique of (D-D+W-S) arrays.	78
Figure 4.28	The contact zone model results given by the DLA technique of (P-D+W) arrays.	79

Figure 4.29 The contact zone model results given by the DLA technique of (P-D+W-S) arrays. 80
Figure 4.30 The contact zone model results given by the joint-inversion of (W+W-S) arrays. 81
Figure 4.31 The vertical dyke model results given by D-D array. 82
Figure 4.32 The vertical dyke model results given by P-D array. 83
Figure 4.33 The vertical dyke model results given by W array. 84
Figure 4.34 The vertical dyke model results given by W-S array. 85
Figure 4.35 The vertical dyke model results given by the DLA technique of (D-D+P-D) arrays. 86
Figure 4.36 The vertical dyke model results given by the DLA technique of (D-D+W) arrays. 87
Figure 4.37 The vertical dyke model results given by the DLA technique of (D-D+W-S) arrays. 88
Figure 4.38 The vertical dyke model results given by the DLA technique of (P-D+W) arrays. 89
Figure 4.39 The vertical dyke model results given by the DLA technique of (P-D+W-S) arrays. 90
Figure 4.40 The vertical dyke model results given by the DLA technique of (W+W-S) arrays. 91
Figure 4.41 The fault model results given by D-D array. 92
Figure 4.42 The fault model results given by P-D array. 93
Figure 4.43 The fault model results given by W array. 94
Figure 4.44 The fault model results given by W-S array. 95
Figure 4.45 The fault model results given by the DLA technique of (D-D+P-D) arrays. 96
Figure 4.46 The fault model results given by the DLA technique of (D-D+W) arrays. 97
Figure 4.47 The fault model results given by the DLA technique of (D-D+W-S) arrays. 98
Figure 4.48 The fault model results given by the DLA technique of (P-D+W) arrays. 99
Figure 4.49 The fault model results given by the DLA technique of (P-D+W-S) arrays. 100
Figure 4.50 The fault model results given by the DLA technique of (W+W-S) arrays. 101
Figure 4.51 The buried bunker model results given by D-D array. 110
Figure 4.52 The buried bunker model results given by P-D array. 111

Figure 4.53 The buried bunker model results given by W array. 112

Figure 4.54 The buried bunker model results given by W-S array. 113

Figure 4.55 The buried bunker model results given by the DLA technique of (D-D+P-D) arrays. 114

Figure 4.56 The buried bunker model results given by the DLA technique of (D-D+W) arrays. 115

Figure 4.57 The buried bunker model results given by the DLA technique of (D-D+W-S) arrays. 116

Figure 4.58 The buried bunker model results given by the DLA technique of (P-D+W) arrays. 117

Figure 4.59 The buried bunker model results given by the DLA technique of (P-D+W-S) arrays. 118

Figure 4.60 The buried bunker model results given by the DLA technique of (W+W-S) arrays. 119

Figure 4.61 Inversion of model resistivity results at Minden, USM, Penang. 124

Figure 4.62 Inversion of model resistivity results at Bukit Bunuh, Perak. 125

LIST OF SYMBOLS

A	Cross-sectional area
C	Current electrode
$\vec{E}$	Electric field intensity
E	East
F	Forward operator
$\vec{J}$	Current density
J	Number of integer
I	Current
k	Geometric factor
km	Kilometre
L	Length of conductor
m	metre
N	North
P	Potential electrode
r	Radius
R	Resistance
V	Potential difference
$\vec{\sigma}$	Conductivity
π	pi (3.14159)
Ω	Ohm
Ω.m	Ohm.meter
ρ	Resistivity
ρ_a	Apparent resistivity
γ	Gamma
%	Percentage
Δ	Changes

LIST OF ABBREVIATIONS

2-D	Two-dimensional
3-D	Three-dimensional
a	Distance between two electrodes
BGS	British Geological Survey
CGAR	Centre for Global Archaeological Research
CR	Compare-R
D	Depth of investigation
DC	Direct current
D-D	Dipole-Dipole
DP	Number of data points
DLA	Data Levels Amalgamation
EHR	Enhancing Horizontal Resolution
et al.	et alia which means “and others”
GPR	Ground Penetrating Radar
i.e.	id est which means “that is”
IM	Inversion model resistivity data point
max	Maximum
n	Ratio **n**(**a**) over **a**
No.	Number
OD	Number of overlapping inversion of model resistivity data
P-D	Pole-Dipole
PO	Percentage of overlapping data point
RES2DINV	Resistivity two-dimensional inversion
RES2DMOD	Resistivity two-dimensional modelling
SAS	Statistical Averaging System
TEM	Transient electromagnetic
USM	Universiti Sains Malaysia
W	Wenner
W-S	Wenner-Schlumberger

PENINGKATAN DALAM RESOLUSI KERINTANGAN BERDASARKAN TEKNIK PENGGABUNGAN DATA

ABSTRAK

Kaedah pengimejan kerintangan 2-D menentukan taburan kerintangan pada bawah permukaan Bumi. Peningkatan dalam kualiti data kerintagan 2-D dilakukan menggunakan kaedah penggabungan tahap data (DLA) berdasarkan pertindihan tahap data dengan kombinasi dua susunatur berlainan. Ojektif pertama kajia ini adalah membangunkan penilaian perbandingan berangka bagi susunatur individu dan kaedah DLA. Tujuan kedua adalah meningkatkan resolusi dengan kaedah DLA bagi dua susunatur berlainan. Tujuan terakhir adalah mengesahsahihkan kaedah DLA bagi dua susunatur berlainan. Dalam usaha untuk mencapai ketiga-tiga objektif, kajian dijalankan dalam tiga fasa yang berlainan. Fasa pertama melibatkan model-model berkomputer 2-D atau dikenali sebagai model-model sintetik dan model lapangan ditunjukkan. Lima model berkomputer berlainan dicipta dan digunakan bagi menyiasat keupayaan pengimejan menggunakan empat susunatur. Dalam fasa kedua, penilaian perbandingan berangka telah diperkenalkan bagi susunatur tunggal dan kaedah DLA. Dua susunatur terbaik dan sesuai ditentukan berdasarkan keputusan penilaian perbandingan berangka. Dalam fasa ketiga, pengesahsahihan bagi kaedah DLA menggunakan dua susunatur yang terbaik dan sesuai diaplikasikan pada tinjauan lapangan yang sebenar. Bedasarkan kepada penilaian perbandingan berangka, bagi model-model berkomputer 2-D dan model lapangan, ia menunjukkan bahawa kaedah DLA bagi dua susunatur Pole-Dipole (P-D) dan Wenner-Schlumberger (W-S) dapat memberikan kualiti data yang baik. Ini disumbangkan oleh jumlah bilangan data

kerintagan ketara berbanding kombinasi yang lain. Pertimbangan kedua adalah peratusan pertindihan data songsangan bagi kaedah DLA adalah baik dengan nilai 79 % keatas. Pertimbangan terakhir adalah kaedah DLA bagi dua susunatur berlainan dapat memberi gambaran sasaran yang baik dalam kedua-dua model kajian. Oleh itu, dua susunatur ini dipilih bagi kajian lapangan di dua tempat berbeza. Keputusan-keputusan pengimejan kerintangan 2-D daripada dua kajian lapangan ditentusahkan dengan data-data lubang bor. Keputusan-keputusan kajian lapangan menunjukkan bahawa kaedah DLA ini adalah berupaya dalam menghasilkan dan meningkatkan resolutsi songsangan bagi kaedah pengimejan kerintangan 2-D. Bagaimanapun, keadaan ini hanya dapat dicapai jika pemilihan susunatur-susunatur yang baik dilakukan. Kesimpulan, kesemua ketiga-tiga objektif kajian telah berjaya dicapai.

ENHANCEMENT IN RESISTIVITY RESOLUTION BASED ON DATA AMALGAMATION TECHNIQUE

ABSTRACT

The 2-D electrical resistivity imaging measured resistivity distribution at the subsurface. Improvement in 2-D resistivity data quality was carried out by the data levels amalgamation (DLA) technique which is based on overlapping data levels with two different arrays combination. The first study objective is to develop the numerical comparative assessment for individual array and the DLA technique of two different arrays. The second objective is to improve resolution using the DLA technique on two different arrays. The final objective is to validate the DLA technique of two different arrays. In order to achieve all three objectives, the study was carried out in three different phases. The first phase involved 2-D computerized models or namely synthetic models and a field model are presented. Five different synthetic models are created and used to investigate the imaging capabilities using four different arrays. In second phase, the numerical comparative assessment is introduced for the individual array and the DLA technique. The two best and suitable arrays were determined based on the numerical comparative analysis results. In phase three, validation of the DLA technique using two best and suitable arrays are applied to the actual field surveys. Based on the numerical comparative assessment for both 2-D computerized models and a field model, it shows that the DLA technique of Pole-Dipole (P-D) and Wenner-Schlumberger (W-S) arrays are able to provide good data quality of image. This is given by a greater total number of apparent resistivity data compared to any other combinations. The second consideration is the percentage of overlapping in inversion

data for the two models using the DLA technique which is also good with a value of greater than 79 %. The last consideration is ability of the DLA technique using two different arrays to resolve image of the known target in both study models. Therefore, these two arrays are chosen for the real field studies in two different areas. The 2-D resistivity imaging results from these two field studies are validated by borehole data. The field study results show that the DLA technique is very capable of producing and enhancing the resolution of inversion of the 2-D resistivity imaging method. However, this condition can only be achieved if proper selection of arrays is made. In conclusion, all of three research objectives were successfully achieved.

CHAPTER 1

INTRODUCTION

1.0 Background

Geophysics is one of the branches of applied earth science which uses principles of physics to study the subsurface. Geophysics has been developing rapidly through the years and has become the main technology in various studies and investigations on the subsurface. Nowadays, it has also helped geoscientists to understand the Earth's phenomena. By measuring different physical parameters and nature of materials in and/or on the Earth, geophysicists are able to study and explore various ground resources such as groundwater, minerals and hydrocarbon. The exploitation of these resources helps many countries generate income including developing countries such as Malaysia.

The 2-D resistivity imaging method is one of the most popular geophysical methods used for the subsurface imaging in environmental and engineering studies. It is chosen for this study due to its ability to provide information of the subsurface structure, water content, depth to bedrock and overburden thickness (Loke 2004; 2014; Reynolds, 1997). In addition, this geophysical method has also been successfully used in complex and noisy geological areas where other geophysical techniques such as seismic refraction/reflection, transient electromagnetic (TEM) and ground penetrating radar (GPR) methods cannot be used for the Earth's subsurface imaging works (Reynolds, 1997).

The purpose of 2-D resistivity imaging is to determine the distribution of subsurface resistivity. 2-D resistivity imaging measurements are taken on the ground surface. From these measurements, estimation of the subsurface true resistivity values can be done by inversion RES2DINV software (Loke, 2001) and MATLAB software (Candansayar, 2008). The subsurface true resistivity values are narrated to many geological parameters: soil mineral, fluid content and water saturation degree in soils/rocks. 2-D resistivity imaging has been used for many years in hydro-geological, mineral exploration and subsurface engineering investigations (Loke, 2004; 2014). More recently, 2-D resistivity imaging method has been used in archaeology, geological structure and groundwater surveys (Martorana et al. 2009; Berge and Drahor, 2009; Muztaza, 2013; Ishola et al. 2014; Ishola, 2015).

With the suitable or right array, the 2-D resistivity imaging method is one of the most suitable geophysical method in engineering and environmental field studies (Dahlin and Zhou, 2004; Loke, 2004; 2014; Neyamadpour et al. 2010a, 2010b, Muztaza, 2013). However, depth and size of the target is very critical in the resistivity study. Resolution is decreased when current travels away from electrodes at the surface (Loke, 199a; Loke, 2014). In addition, poor scalability of electrode spacing, wrong array selection and poor ground contact lead to bad interpretation and improper use of the 2-D resistivity imaging method.

In electrical resistivity surveys, high resolution, reliable and good imaging depends on the choice of electrode configuration or namely array. The electrode configuration used should provide adequate information about the Earth's model (Dahlin and Zhou, 2004). The selection of the most appropriate array has continued to be a topic of discussion among researchers in view of their merits and limitations (Olayinka and Yaramanci, 1999). The debate about how to select the most

appropriate electrode array has been a long and continuing history in electrical resistivity survey (Candansayar, 2008).

Several studies have been carried out regarding the performance of various arrays. There are many types of arrays to be used for data acquisition in field survey. Some of the common arrays are Dipole-Dipole (D-D), Pole-Dipole (P-D), Wenner (W) and Wenner-Schlumberger (W-S) (Candansayar, 2008; Reynolds, 1997; Chambers et al., 1999; Storz et al., 2000). It is generally recognized that W and W-S arrays are less sensitive to noise and high vertical resolution (Dahlin and Zhou, 2004). Roy and Apparao (1971) and Barker (1979) studied the depth of investigation of different array types. The resolution and accuracy of inverted data sets have been investigated by various researchers (Sasaki, 1992; Dahlin and Zhou, 2004).

1.1 Problem statements

At present, data processing techniques using only one type of resistivity array have a few disadvantages such as low horizontal coverage, low vertical coverage, low resolution, low signal strength, high noise level, and shallow penetration depth (Loke, 2004; 2014). D-D, P-D and W-S arrays are easily contaminated by noise compared to W arrays (Dahlin and Zhou, 2004). This is due to a good signal strength by W array compared to other arrays. D-D array has low vertical resolution compared to P-D, W and W-S (Barker, 1979).

D-D array is very sensitive to resistivity horizontal changes. However, this array is insensitive to resistivity vertical changes (Loke, 2004; 2014). P-D array has good horizontal coverage in 2-D resistivity imaging (Loke, 2004; 2014). This array

also has good depth of investigation compared to other arrays (Muztaza, 2013). W array is sensitive to resistivity vertical changes. However, this array is less sensitive to resistivity horizontal changes in subsurface. W-S array is moderately sensitive both vertical and horizontal changes in resistivity (Loke, 2004; 2014). The horizontal data coverage of W-S array is wider than W array (Loke, 2004; 2004).

To overcome these problems, the numerical comparative assessment is carried out for individual array and the DLA technique for two different arrays. The DLA technique used in this study is lightly similar to the joint-inversion technique. The numerical comparative assessment is carried out for three main parameters. These parameters are also vital in producing high resolution in the 2-D resistivity imaging method. Based on the numerical comparative assessment and the DLA technique, selection of the two best and suitable arrays can be made for the real field studies to get the 2-D resistivity imaging results. Borehole records were used as geological references in interpretation work.

1.2 Research objectives

The objectives in this research are:

i. To compare the numerical comparative assessment for individual array and the DLA technique of two different arrays.
ii. To improve resolution in data processing using the DLA technique on two different arrays.
iii. To validate the DLA technique of two different arrays to provide significant improvement in 2-D resistivity imaging data quality.

1.3 Motivation and research novelty

A previous study by as de la Vega et al. (2003) concluded that the joint-inversion technique of W and D-D arrays can improves the depth of investigation. Neyamadpour et al. (2010a) claimed that the joint-inversion technique of W and D-D arrays can be highly useful for cavity detection. However, Berge and Drahor (2003) claimed that the combination or joint-inversion technique of different arrays would not be useful in every situation. Athanasiou et al. (2007) indicated that algorithm used in combined weighted inversion does not necessarily gives optimum results. It shows that, there are many debates in the joint-inversion technique of the 2-D resistivity imaging. Critical comments on previous studies on the joint-inversion technique in the 2-D resistivity imaging method are carried out in Chapter 2.

This research aims to modify the conventional resistivity data processing technique. The originality of this research lies in the numerical comparative assessment between the results obtained using individual array and the DLA technique for the two best and suitable different arrays. The numerical comparative assessment was developed and carried out with respect to (i) number of apparent resistivity data, (ii) percentage of overlapping inversion model data and lastly (iii) ability to resolve the known target. This novel approach allows the 2-D resistivity imaging method to be carried out on the two best and suitable arrays rather than using three or four arrays. In addition, this approach only focused on the use of geophysical inversion software rather than using non-geophysical software. The DLA technique for these two suitable arrays is a useful approach in data processing strategy to enhance resolution of the 2-D resistivity imaging method.

1.4 Layout of thesis

In general, the thesis content is systematized as follows.

In Chapter 1, the background of this research is introduced. Problem statements and objectives to be achieved in this research are highlighted. Furthermore, motivation and research novelty as well as the layout of thesis are presented in this chapter.

In Chapter 2, the general method and principle of electrical resistivity method used are discussed. Several previous studies done by other researchers using geophysical methods applied in environmental and engineering problems are also discussed. In addition, recent development of resistivity method and critical comments on the joint-inversion technique are also discussed to give an overview as a stepping stone for this research.

In Chapter 3, research methodology is discussed on the development of the DLA technique. This chapter continues to discuss five different 2-D computerized models and a field model. The development of the numerical comparative assessment is presented for the selection of the two best and suitable arrays for the actual field studies. In addition, geological setting and survey geometry for two field study areas are discussed.

Chapter 4 discusses the study results according to the flow of research; the 2-D computerized models, a field model and the numerical comparative assessment. Based on the conclusion of these two model tests and the numerical comparative assessment, two best and suitable arrays are chosen to be used for the real field

studies in two different areas. The discussion is followed by the results from these field studies.

Lastly, Chapter 5 discusses the conclusion of the 2-D resistivity imaging method using the DLA technique in data processing. The summary of the whole research together with the advantages of the DLA technique are also discussed. Finally, some recommendations for the future research are proposed.

CHAPTER 2

LITERATURE REVIEWS

2.0 Introduction

Geotechnical studies are normally related to soils or rocks properties, man-made structures, foundations and environmental works. Geophysical studies are capable of providing supporting relevant imaging (data) in order to reduce operation cost and time effective. Using drilling borehole only provides information in discrete locations and incurs high cost to study the subsurface characterizations. Geophysical methods such as the 2-D resistivity imaging method can be used to identify the bedrock depth and overburden (soils) materials (Samsudin et al. 1998). In addition, this geophysical method is capable of detecting or imaging some near-surface structures such as sinkholes, faults and boulders. Selection of suitable and appropriate geophysical method is closely related to the objective of a study or project and the site's conditions (Reynolds, 1997). Geophysical methods allow the ground subsurface conditions to be examined indirectly, quickly, reliably and cost effectively with sufficient results. These geophysical methods utilize different physical properties of the ground's material to study the subsurface structures as described by Samsudin et al. (1998). Geophysical methods are routine procedures to delineate geological structures and other subsurface phenomena (Dahlin, 1996). Proper usage of these geophysical methods could leads to an increase in resolution of the ground subsurface model or pseudosection.

The 2-D resistivity imaging method is used to detect groundwater and subsurface characterizations (Araffa et al. 2015). IP method is normally used in waste landfills mapping while self-potential method is normally used in seepage tracks mapping (Loke, 2004). The electrical method's applications in environmental and engineering studies are widely used for many aspects such as slope monitoring, soil characterizations as well as mineral and groundwater explorations (Samsudin et al. 1998; Samsudin et al. 2008; Nordiana et al. 2012; Seaton and Burby, 2000).

2.1 Electrical resistivity theory

The general partial differential equation governing electrical resistivity method can be derived from basic electrical principle. The fundamental physical law used in electrical resistivity method is Ohm's Law that governs the flow of current in the ground. Equation 2.1 shows Ohm's Law in vector form for current flow in a continuous medium:

$$\vec{J} = \vec{\sigma}\vec{E} \tag{2.1}$$

where $\vec{\sigma}$ is conductivity of the medium, $\vec{J}$ is current density and $\vec{E}$ is electric field intensity. In practice, what is measured is an electric field potential. Note that for electrical resistivity method, medium resistivity, $\vec{\rho}$ is equal to a reciprocal of the conductivity, and $\vec{\rho} = 1/\vec{\sigma}$, is more commonly used. In 1827, a German scientist, Georg Simon Ohm found that an electrical current, (I) in a conducting wire is proportional to potential difference, (V) across it (Equation 2.2).

$$V \alpha I \tag{2.2}$$

To grasp the theory of resistivity, potential difference, (V) and current, (I) that flows through the circuit are measured. Thus, an increase in resistance, (R) value across the circuit will result in the dropping of current, (I) (Equation 2.3). It shows that current is inversely proportional to resistance.

$$I = \frac{V}{R} \tag{2.3}$$

The potential difference is measured experimentally using a voltmeter while the current is measured using an ammeter. The SI unit for resistance is volts per ampere or Ohm, (Ω). The resistivity can be calculated using Equation 2.4.

$$\rho = R \ \frac{A}{L} \tag{2.4}$$

where:

ρ = Resistivity of the conductor material (Ω.m)

R = Resistance

A = Cross-sectional area (m^2)

L = Length of the conductor (m)

For a homogeneous media with one electrode, the potential will separate radially outwards from the current source where area, (A) will be a half sphere, ($2\pi r^2$) with radius, (r). Equation 2.4 is rewritten as Equation 2.5.

$$\rho = k\,R \tag{2.5}$$

where, $k = 2\pi r$ for the half sphere. Equation 2.5 consists of two parts. The first part is resistance, (R) and the second part is geometric factor, (k) which describes the geometry of electrode configuration.

2.2 Basic concept of 2-D resistivity imaging

A fundamental property of any volume of material is its resistance measured in the unit of Ohm. The resistance is defined as the material's opposition to the flow of electrical current (Reynold, 1997). Resistivity (in unit of Ω.m) is related to this property and is expressed as resistance through a distance, which makes it independent of material geometry (Reynold, 1997).

Resistivity is considered as functions of rock porosity, volumetric fraction of saturated pores and resistivity of pore water (Archie, 1942). In many cases, it is the pore fluid of rock that accounts for the overall resistivity signature rather than the host rock (Lowrie, 1997). In 2-D resistivity imaging measurement, the basic procedure is to establish a subsurface distribution of resistivity by injecting current into the underground between two current electrodes planted on ground surface. The resulting potential difference are measured between two potential electrodes in a line or grid (Ramirez et al., 1993). The ground (Earth) can be considered as one component of an electrical circuit known as the resistor. An interpretation of the measured parameters yield information about the electrical conductivity beneath, the ground's surface.

The 2-D resistivity imaging measurements for a homogeneous medium are normally made by injecting current into the ground through two current electrodes (C1 and C2) and measuring the resulting voltage difference between two potential electrodes (P1 and P2) (Figure 2.1). From the current, (I) and voltage, (V), an apparent resistivity, (ρ_a) value is calculated (Equation 2.6).

$$\rho_a = \frac{kV}{I} \tag{2.6}$$

where, k is the geometric factor which depends on the arrangement of the four electrodes. Figure 2.1 shows common electrodes array for resistivity measurement.

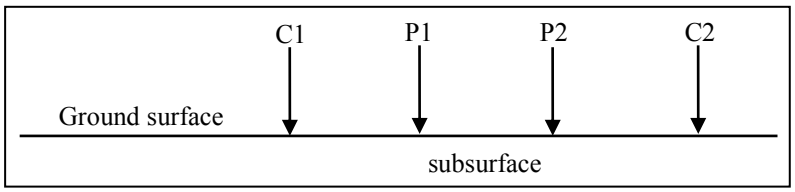

Figure 2.1: Common electrodes array for resistivity measurement.

Therefore, for an inhomogeneous case, the resistivity meter normally measures resistance value, (R) as given by Equation 2.3. In practice, the apparent resistivity value is calculated by Equation 2.7.

$$\rho_a = k\,R \tag{2.7}$$

The geological structures of the Earth's subsurface are inhomogeneous and the resistivity, that is collected, does not represent the true resistivity, but it represents an apparent resistivity (Paul, 2007). The relationship between the "apparent" and "true" resistivity values is a multiplex connection. In order to determine true subsurface resistivity values from its apparent values, an inversion using a computer program is needed for measured apparent resistivity data (Loke, 1999a; Loke, 2014).

2.3 The general four-electrode method

Consider an arrangement which consists of a pair of current electrodes and a pair of potential electrodes. Figure 2.2 shows a diagram of the four-electrode method. This arrangement will be used to illustrate the current flow into the ground.

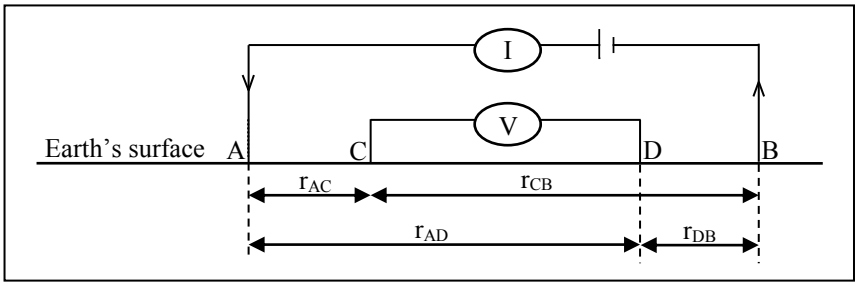

Figure 2.2: Arrangement of four-electrode in electrical resistivity method.

The current electrodes A and B act as the source and sink. At the detection electrode C, potential due to the source A is $+\rho I/(2\pi r_{AC})$, while potential due to the sink B is $-\rho I/(2\pi r_{AC})$. The combined potential at C is given by Equations 2.8–2.10.

$$V_C = \frac{\rho I}{2\pi r_{AC}} + \left(-\frac{\rho I}{2\pi r_{CB}} \right) \tag{2.8}$$

$$V_C = \frac{\rho I}{2\pi r_{AC}} - \frac{\rho I}{2\pi r_{CB}} \tag{2.9}$$

$$V_C = \frac{\rho I}{2\pi} \left(\frac{1}{r_{AC}} - \frac{1}{r_{CB}} \right) \tag{2.10}$$

This is similar to the resultant potential at D. This is given by Equation 2.11.

$$V_D = \frac{\rho I}{2\pi}\left(\frac{1}{r_{AD}} - \frac{1}{r_{DB}}\right) \tag{2.11}$$

The potential difference measured by a voltmeter connected between C and D is given by Equation 2.12–2.14.

$$V = V_C - V_D \tag{2.12}$$

$$V = \frac{\rho I}{2\pi}\left(\frac{1}{r_{AC}} - \frac{1}{r_{CB}}\right) - \frac{\rho I}{2\pi}\left(\frac{1}{r_{AD}} - \frac{1}{r_{DB}}\right) \tag{2.13}$$

$$V = \frac{\rho I}{2\pi}\left[\left(\frac{1}{r_{AC}} - \frac{1}{r_{CB}}\right) - \left(\frac{1}{r_{AD}} - \frac{1}{r_{DB}}\right)\right] \tag{2.14}$$

All quantities in this Equation (2.14) can be measured at the ground surface except the resistivity value, which is given by Equation 2.15.

$$\rho = 2\pi \frac{V}{I}\left[\frac{1}{\left(\frac{1}{r_{AC}} - \frac{1}{r_{CB}}\right) - \left(\frac{1}{r_{AD}} - \frac{1}{r_{DB}}\right)}\right] \tag{2.15}$$

This ρ is called apparent resistivity. Therefore, Equation 2.15 can be rewritten as Equation 2.16.

$$\rho_a = 2\pi \frac{V}{I}\left[\frac{1}{\left(\frac{1}{r_{AC}} - \frac{1}{r_{CB}}\right) - \left(\frac{1}{r_{AD}} - \frac{1}{r_{DB}}\right)}\right] \tag{2.16}$$

Then, Equation 2.16 can be rearranged as Equation 2.17 to get the final equation as Equation 2.18. Therefore, Equation 2.18 is equal to Equation 2.6 and Equation 2.19 is equal to Equation 2.7.

$$\rho_a = 2\pi \left[\frac{1}{\left(\frac{1}{r_{AC}} - \frac{1}{r_{CB}}\right) - \left(\frac{1}{r_{AD}} - \frac{1}{r_{DB}}\right)} \right] \frac{V}{I} \tag{2.17}$$

$$\rho_a = k \frac{V}{I} \tag{2.18}$$

$$\rho_a = k\, R \tag{2.19}$$

2.4 Selecting electrode array for 2-D resistivity survey

The 2-D resistivity survey has remained an essential tool for over two decades (Dahlin, 1996; Seaton and Burby, 2000; Loke, 2014) as geophysical investigations are used for hydrogeology, subsurface exploration, mining, geotechnical engineering and archaeological prospecting. The success of the 2-D resistivity imaging method in mapping Earth's subsurface structures depends on other factors in the choice of suitable electrode array.

Among the several electrode arrays that are commonly used in 2-D resistivity imaging are standard arrays; Dipole-Dipole (D-D), Pole-Dipole (P-D), Wenner (W) and lastly Wenner-Schlumberger (W-S) (Chambers et al., 1999; Storz et al., 2000). The difference between these array types lies in separation between the electrodes pairs that provide variation or differences in the geometric factor for each electrode

array (Loke, 2004; Loke et al., 2010). In view of advantages and limitations of one electrode array over another, several researchers have investigated electrical resistivity survey capabilities of different electrode arrays by comparison (Dahlin and Zhou, 2004; Perren, 2005, Putiska et al., 2012; Alwan, 2013).

2.4.1 D-D array

In D-D array (Figure 2.3), a pair of potential electrode are on the outside of a pair of current electrode. Each pair of electrode has a constant electrode separation (**a**) and the distance between two innermost electrodes is (**na**). The measured apparent resistivity, ρ_a is given by Equation 2.20.

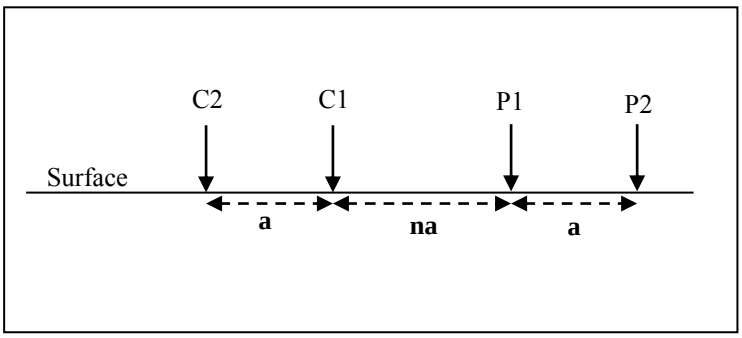

Figure 2.3: Electrode's arrangement for D-D array.

$$\rho_a = \pi na(n+1)(n+2)R \qquad (2.20)$$

where;

n = Ratio of **n**(**a**) over **a**

a = Distance between two electrodes

R = Resistance (Ohm)

2.4.2 P-D array

P-D array (Figure 2.4) is an electrical array for 2-D resistivity imaging that contains four co-linear electrodes with one of the current electrodes (which acts as the source) positioned at an infinity distance. Usually, it is positioned at approximately five to ten survey depth (Loke, 2001). The other current electrode is placed in vicinity of a pair of potential (receiver) electrode. This geometry is used because it reduces the distortion of equipotential surfaces (Smith, 1986). The measured apparent resistivity, ρ_a is given by Equation 2.21.

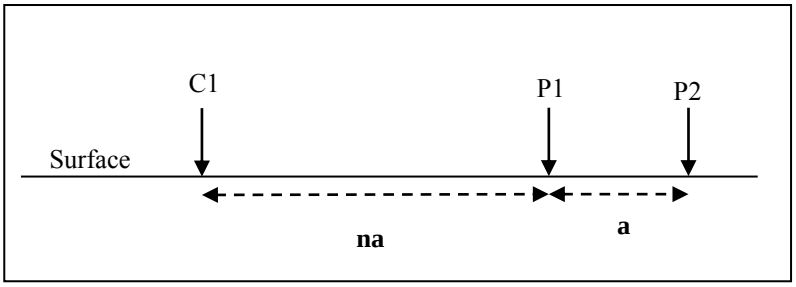

Figure 2.4: Electrode's arrangement for P-D array.

$$\rho_a = 2\pi na(n+1)R \qquad (2.21)$$

where;

n = Ratio of **n**(**a**) over **a**

a = Distance between two electrodes

R = Resistance (Ohm)

2.4.3 W array

In W array (Figure 2.5), a pair of current electrodes and a pair of potential electrodes are arranged collinearly and separation between adjacent four electrodes are equal. This separation is denoted by (**a**). Due to simplicity in its geometry, this array is often used in electrical resistivity survey. In normal electrical resistivity sounding measurement using W array, distance (**a**) is increased step by step, while keeping middle-point of electrodes fixed. The measured apparent resistivity, ρ_a is given by Equation 2.22.

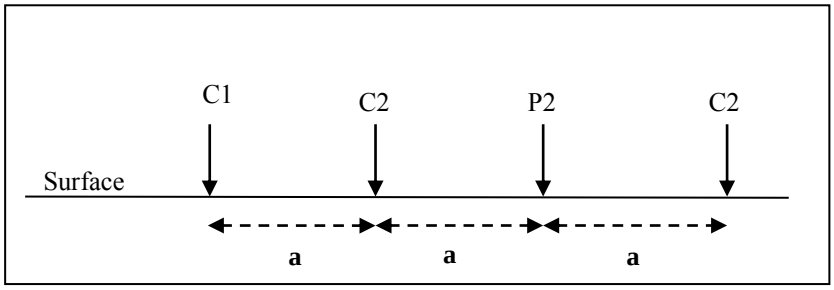

Figure 2.5: Electrode's arrangement for W array.

$$\rho_a = 2\pi aR \qquad (2.22)$$

where;

a = Distance between two electrodes

R = Resistance (Ohm)

2.4.4 W-S array

W-S (Figure 2.6) array is also one of the most commonly used array for the ground subsurface investigation. This array has a pair of current electrodes and a pair of potential electrodes are arranged collinearly. In this array, separation between the pair of current electrodes is much larger than separation between the pair of potential electrodes. In this array, the electrode layout for the first data level (**n**=1) is same as W array. The measured apparent resistivity, ρ_a is given by Equation 2.23.

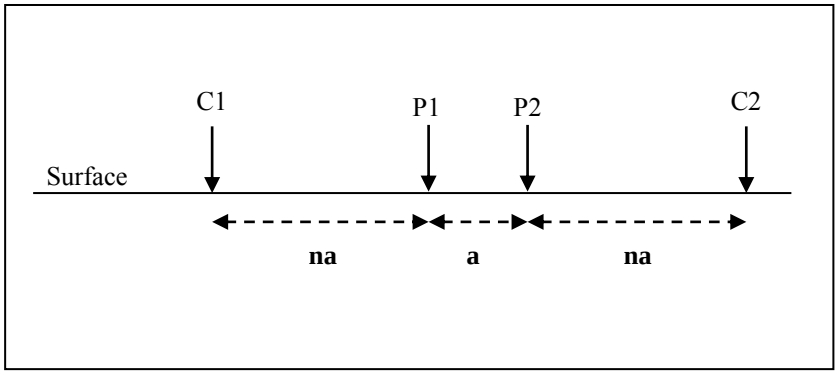

Figure 2.6: Electrode's arrangement for W-S array.

$$\rho_a = \pi na(n+1)R \qquad (2.23)$$

where;

n = Ratio of **n**(**a**) over **a**

a = Distance between two electrodes

R = Resistance (Ohm)

2.5 Electrode arrays

An arrangement of the electrodes is called an electrode array. The apparent resistivity value depends on the geometry of the electrodes (geometric factor, k) (Reynolds, 1997). The geometric factor depends on the position of electrodes in the array. Resistivity imaging employs different types of electrode arrays.

According to Norman and Fujita (1997), the most common arrays used in resistivity imaging survey are W, D-D and W-S. Choosing the right array for a resistivity survey is important for two reasons. The first one is that for each array, there are varying degrees of advantages and disadvantages when compared with other arrays. The second reason is that the resistivity image of the same structure is different when produced by a different array.

Choosing the appropriate array depends on the survey's objective. Moreover, choosing the appropriate array requires some considerations such as depth of the object, vertical and horizontal changes of the subsurface and signal strength (Loke, 2001; Dahlin and Zhou, 2004). Figure 2.7 shows some common arrays used in resistivity surveys together with their geometric factors.

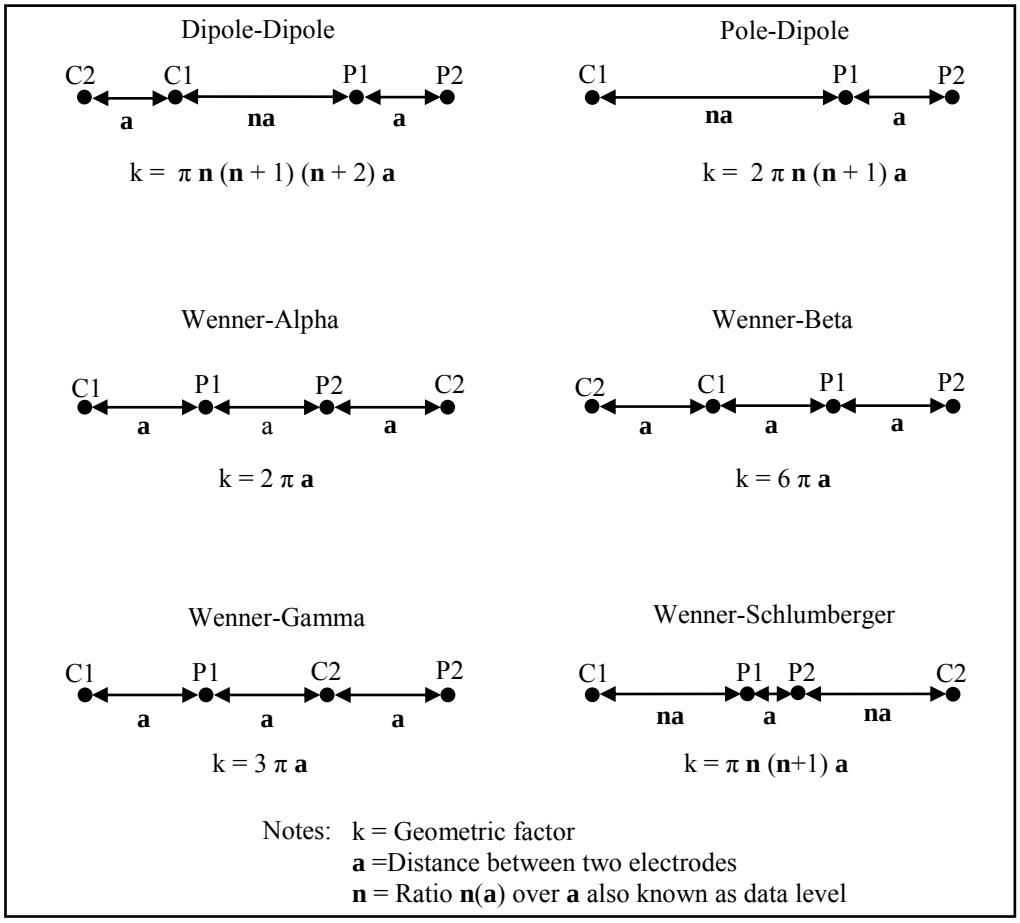

Figure 2.7: Common arrays used in resistivity and their geometric factors (ABEM, 2006).

2.6 Inversion of resistivity data

The objective of electrical resistivity inversion is to find a model which adequately reproduces the observed data (Oldenburg, 1978). In recent years, several methods have been developed for the direct interpretation of the 2-D electrical resistivity data. Since most of the direct current electrical resistivity problems are non-unique, iterative methods are commonly used for practical inversion of the data (Jupp and Vozoff, 1975). The iterative method successively improves the model parameters by reducing the error between the model response and observed data.

The ridge regression method (Imam, 1975) has been used by other researchers (Rijo et al., 1977; Petrick, et al., 1977) in inversion of one-dimensional electrical resistivity sounding data. This method was extended by Pelton et al. (1978) to invert electrical resistivity and induced polarization data over two-dimensional structure. This method requires many forward modelling evaluations for each ridge regression inversion as well as large memory space. Furthermore, this method gives an erratic electrical resistivity distribution when many model layers are used in the inversion (Constable et al., 1987).

Tripp et al. (1984) used the transmission surface analogy to generate the initial model of D-D electrical resistivity data. For noisy data, the resulting model after inversion is diverged from the real model. Shima (1990, 1992) used the alpha centre method for the 2-D inversion of surface and cross-hole electrical resistivity data. The main disadvantage of the alpha centre method is that it is not suitable for complex structures with high contrast and sharp boundary.

The effect of topography plays a significant role in the inversion scheme (Fox et al., 1980; Spiegel et al., 1980). Tong and Yang (1990) proposed a finite element forward modelling scheme that takes into account topographic feature in the inversion of electrical resistivity data. The Zohdy-Barker method (Barker, 1992) uses a modification of Zohdy's optimization technique (Zohdy, 1989) to convert the 2-D data pseudosection. Although improvements were made by Loke and Barker (1995a) to overcome problems of the relatively slow convergence and instability, this method does not converge to the real model for complex geological structures.

It is obvious from the literature that most of these algorithms are implemented on mini or mainframe or workstation computers. Many electrical

resistivity surveys are carried out by small companies for mineral, hydrogeological and engineering purposes. The computing resources needed may not be available, and it would not be practical to carry out the inversion during the field survey or data acquisition.

The recent improvements to data acquisition equipment for electrical resistivity surveys require a similar development of more sophisticated inversion algorithms to fully utilize electrical resistivity data (Griffiths and Turnbull, 1985; Griffiths et al., 1990). Loke and Barker (1995b, 1996) have developed a fast inversion algorithm whereby a 2-D structure can be modelled on a computer during field survey or data acquisition of electrical resistivity.

2.7 Previous studies

Several case studies are discussed in this chapter, which involve the application of electrical resistivity with other geophysical methods and electrical resistivity with some geotechnical engineering methods. These previous geophysical studies are related to engineering and environmental perspectives. Furthermore, the discussion includes recent developments of 2-D resistivity imaging method by various researchers.

Samsudin et al. (2008) combined 2-D resistivity imaging and seismic reflection survey with hydro-chemical methods. The study was carried out to map saline water intrusion into coastal groundwater aquifers in Kelantan, Malaysia. Integration of all results apart from delineating the subsurface geologic units also indicated the extent of presence of total dissolved solids among other components in the water.

Saad et al. (2011) presented integrations between 2-D electrical resistivity and seismic refraction methods to study shallow subsurface. The study was carried out in Selangor, Malaysia.

Giang et al. (2013) presented results of geophysical methods such as vertical electrical sounding, very low frequency, seismic refraction and electrical resistivity imaging. The work's purpose was to locate the aquifers and to assess the hydro-geological conditions for groundwater potential. The research location is in the industrial zones of North Hanoi, Vietnam.

Geophysical methods-seismic refraction, electrical resistivity tomography and microgravity were applied to Dead Sea sinkhole problem in the Ein Gedi area at an earlier stage of the sinkhole development. The methods allowed the determination of the sinkhole formation mechanism and localization of the hazardous sinkhole zones. This study was conducted by Ezersky et al. (2013). The suitability of the combined microgravity and resistivity tomography to detect and characterize caves deeply buried in limestone is proposed by Martinez-Moreno et al. (2013). At the investigation site, microgravity, electrical resistivity and IP data was collected along four profiles.

Hamdan and Vafidis (2013) presented the development of joint-inversion strategies. The research was conducted to improve on electrical resistivity and seismic velocity models for delineating saline water zones in karst geological formations. The 2-D resistivity imaging method was carried out to provide a better means of bridging information. This electrical resistivity method is used to map geotechnical properties of the subsurface. The study was presented by Rucker and Noonan (2013) at Panama Canal. Dahlin et al. (2013) proposed calibration of